Available online at www.sciencedirect.com
ScienceDirect
Trans. Nonferrous Met. Soc. China 28(2018) 1141−1148
Transactions of Nonferrous Metals Society of China
www.tnmsc.cn

Fabrication of porous FeAl-based intermetallics via thermal explosion

Ya-nan LIU[1,2], Zhi SUN[1], Xiao-ping CAI[1], Xin-yang JIAO[1], Pei-zhong FENG[1]

1. School of Materials Science and Engineering, China University of Mining and Technology, Xuzhou 221116, China;
2. School of Chemical Engineering and Technology,
China University of Mining and Technology, Xuzhou 221116, China

Received 21 February 2017; accepted 24 May 2017

Abstract: Porous FeAl-based intermetallics were fabricated by thermal explosion (TE) from Fe and Al powders. The effects of sintering temperature on phase constitution, pore structure and oxidation resistance of porous Fe−Al intermetallics were systematically investigated. Porous Fe−Al materials with high open porosity (65%) are synthesized via a low-energy consumption method of TE at a temperature of 636 °C and FeAl intermetallic is evolved as dominant phase in sintered materials at 1000 °C. The porous materials are composed of interconnected skeleton, large pores among skeleton and small pores in the interior of skeleton. The interstitial pores in green powder compacts are the important source of large pores of porous Fe−Al intermetallics, and the in-situ pores from the melting and flowing of aluminum powders are also significant to the formation of large pores. Small pores are from the precipitation of Fe−Al intermetallics particles. In addition, the porous specimens exhibit high resistance to oxidation at 650 °C in air.

Key words: Fe−Al intermetallics; porous material; thermal explosion; phase transition

1 Introduction

In the past decades, research on inorganic porous materials has increased considerably due to their important applications in environmental protection and industrial filtration [1]. The current inorganic porous materials are divided into two parts: porous ceramics and porous metals. Porous ceramics, which are characterized by high melting points, high corrosion and wear resistance, low thermal mass and thermal conductivity, are widely applied in many fields, such as catalyst supports, wastewater treatment, heat insulation and metal filtration [2,3]. However, the intrinsic brittleness, low thermal shock resistance and poor weld ability have limited their applications. Though porous metals have advantages over ceramics, like superior toughness and weld ability, they exhibit poor resistance to oxidation and corrosion in acid/alkali environment, and low strength at elevated temperature [4,5]. As a consequence, it is badly in need of a novel material that possesses the merits of metals and ceramics. Fe−Al intermetallics have been of great interest on account of their unique combinative properties of both ceramics and metals characteristics, such as low density, low production cost, excellent corrosion resistance and oxidation resistance [6−8]. Therefore, porous Fe−Al intermetallics could work as potential materials for purification and separation in rugged environment.

Up to now, various technological routes have been proposed to prepare porous Fe−Al intermetallics. CHOJNACKI et al [9] have achieved FeAl intermetallic foam with the addition of magnesium hydride, acknowledged to the decomposition of MgH_2 with H_2 in situ evolution. ŁAZINSKA et al [10] have obtained FeAl intermetallic foam using NaCl as the pore former. Nevertheless, in such situation remaining MgH_2 or NaCl may affect the mechanical properties and corrosion resistance performance of Fe−Al intermetallics and/or have a negative effect on the furnace. Moreover, organic compound aided sintering is a quite popular approach of metallic foams formation. KARCZEWSKI et al [11−13] have prepared intermetallic Fe−Al foam by powder metallurgy with the organic pore former (crystalline oxalic acid, palmitic acid, cholesteryl myristate). Whereas some gases will actually release into the air

Foundation item: Project (51574241) supported by the National Natural Science Foundation of China; Project (51611130064) supported by the Bilateral Project of NSFC-STINT; Project (2015QN004) supported by the Program for Innovation Research Team of China University of Mining and Technology

Corresponding author: Pei-zhong FENG; Tel: +86-516-83591879; Fax: +86-516-83591870; E-mail: fengroad@163.com

DOI: 10.1016/S1003-6326(18)64737-5

because of the decomposition of organic, which may be harmful to the environment. GAO et al [14] have fabricated porous Fe−Al intermetallics based on Kirkendall effect through sintering process accompanied with a heating rate of 1 °C/min in the temperature range of 550−650 °C. It is a high-energy consumption fabrication route. However, the combustion synthesis (CS) provides a simple, economic and highly efficient method for fabricating intermetallics [15−18]. And two reaction modes are involved in CS procedures, self-propagating high-temperature synthesis (SHS) and thermal explosion (TE). During the SHS process, the reaction is initiated by heating one end of the reactant compact. Previous study [14,19] showed that it is difficult to preserve the final product with the desirable shapes; whereas in the TE process, the reaction is ignited by heating the entire reactant compact. In general, the TE is conducted in a furnace where all of the reactants are heated simultaneously. As a consequence, TE can avoid the deformation and cracks of the specimen during the sintering process [20].

In this work, a simple and energy-saving approach has been explored to fabricate porous Fe−Al intermetallics with near-net-shape by TE reaction. The effects of sintering temperature on phase constitution, pore structure and oxidation resistance of Fe−Al intermetallics have been systematically investigated. Besides, the pore forming mechanism has also been discussed.

2 Experimental

Elemental Fe (<50 μm, 99.6% purity) and Al (<50 μm, 99.0% purity) powders were employed as reactant materials. Fe and Al powder mixture with 1:1 in molar ratio was homogenized in a planetary ball mill (QM-ISP 2CL, Nanjing NanDa Instrument Plant, China) at 450 revolution/min for 2 h using agate balls in agate vessels at ambient temperature. The mass ratio of ball to powders was 1:1. Absolute ethanol was used as milling medium. The mixed powder was dried completely in an oven for 24 h at a stable temperature of 40 °C. The dried mixtures were uniaxially pressed into green compacts under a pressure of 200 MPa, with a diameter of ~16 mm and a height of ~2 mm, and then the as-pressed discs were sintered in a vacuum furnace at a constant heating rate of 10 °C/min. To study the effects of sintering temperature on phase transition and pore structure evolution, the specimens were sintered at temperatures of 500, 550, 600, 650, 700, 800, 900 and 1000 °C for 1 h. Extensive experiments have found that the specimens exhibited a sharp volume expansion when sintered at 650 °C. With the same heating rate, we conducted the experiment in a tube furnace in a flowing argon atmosphere to identify the appearance of TE. During this procedure, thermocouple wires (WRe3-WRe25 with a diameter of 0.1 mm) were placed between two discs to record explosion temperatures with a frequency of 100 Hz.

The open porosity was measured based on Archimedes principle [21,22]. Sintered specimens were polished to study optical morphology. The final products ground to powders were identified by X-ray diffractometry (XRD) on a Bruker D8 ADVANCE X-ray diffraction machine with Cu target (λ=0.15406 nm), operating at 40 kV and 150 mA. Quanta 250 scanning electron microscope (SEM) was employed to examine the pore structure. The optical metallography of the polished specimens was performed on an Olympus optical microscope (Japan, PMG 3). The thermal analysis was carried out on thermogravimetry differential scanning calorimeter (TG−DSC: STA449F3, Netzsch, Germany) under argon atmosphere with a heating rate of 10 °C/min.

The oxidation experiments were conducted at 650 °C for 4 cycles and duration of 96 h under air atmosphere. The mass of porous Fe−Al monoliths was measured before and after each cycle. The oxidation kinetics of the porous Fe−Al materials was determined by measuring the change in mass every 24 h as a function of the exposure time.

3 Results and discussion

3.1 Characteristics of TE reaction

Figure 1 shows DSC curve of a Fe−50Al pellet heated at a heating rate of 10 °C/min. In the Fe−Al system, the exothermic reactions take place during the sintering of Fe−Al compounds from elemental powders, as can be seen from Fig. 1. Two exotherms can be seen with the onset of exothermic reactions at 574 and 643 °C. The first exothermic peak is more diffuse, whereas the second peak is shaper. This means that the mechanism governing the first peak is more time-dependent [23], where the reaction is in the solid state. Compared with the heating rate of 1 °C/min in the temperature range of 550−650 °C for Fe−Al compounds conducted by GAO et al [14], a higher heating rate decreases the time for diffusion of the atoms and consequently the reaction is not violent [24]. At the same time, the second peak is more instantaneous, indicating that the reaction of Fe−Al compound is violent and causes a large amount of heat emission. Also, the exothermic nature of the reaction can be inferred from the data in Fig. 2, which shows the temperature−time profile in an experiment performed at a heating rate of 10 °C/min. The critical temperature at which combustion occurs is defined as the ignition temperature (T_i). The

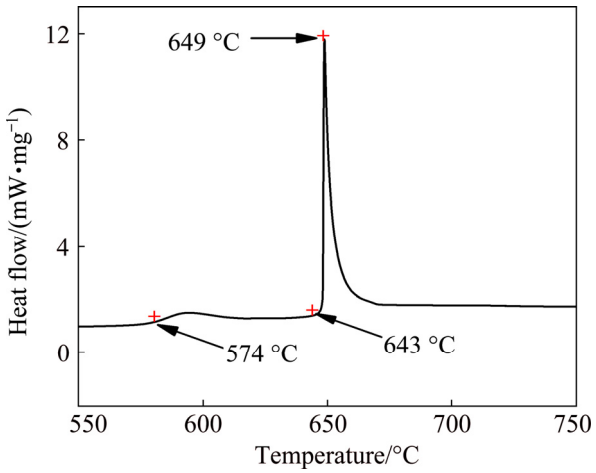

Fig. 1 DSC curve of Fe−50Al mixture at heating rate of 10 °C/min

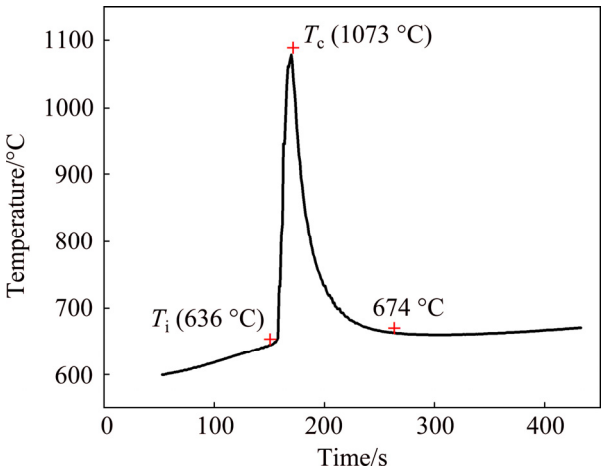

Fig. 2 Combustion temperature−time profile of Fe−Al powder compact during sintering

maximum temperature of the TE reaction is denoted as the combustion temperature (T_c). As shown in Fig. 2, the reaction is ignited when the furnace temperature reaches the T_i (636 °C), leading to a sharp rise to T_c (1073 °C). This is TE reaction that occurs transiently like an explosion, during which large amount of heat releases, resulting in a rapid increase in the temperature of specimen to T_c (1073 °C) in a short time (within 6 s). At the end of TE, there is no enough heat available to maintain the temperature of the specimen at 1073 °C. Therefore, due to the large temperature gradient between the specimen and the furnace, the specimen cools rapidly to 674 °C, which means that TE process has finished. However, this observation is different from those results highlighting the role of melt formation in triggering the combustion reaction [25]. In the present case, it is clearly seen from Fig. 2 that the ignition temperature is about 636 °C, which is below the melting point of Al (660 °C). The explanation is that an amount of heat is given to the samples due to the Fe_2Al_5 formed through the solid−solid reaction between Fe and Al, causing enough heat accumulation in the sample and initiating combustion at lower temperatures [23]. The dramatic increase in the sample temperature (1073 °C) can be attributed to the exothermic reaction occurring between Fe and Al powder mixture, which will be referred later.

3.2 Phase transformation

To understand the effect of temperature on the formation of FeAl as well as to find pore forming mechanism, the samples are heated to 500, 550, 600, 650, 700, 800, 900 and 1000 °C and held for 1 h, and then cooled down (furnace cooling). Figure 3 shows the XRD patterns of the specimens with sintering temperature increasing from 500 to 1000 °C. As illustrated in Fig. 3, the results show that sintering temperature has a strong influence on the phase composition of the specimens. Only Fe and Al phases are detected, indicating that no reaction, at least no detectable reaction between Fe and Al takes place when the sintering is carried out at or below 500 °C. With increasing temperature to 600 °C, the newly formed phase Fe_2Al_5, reactant Fe and Al exist, which shows that the formation of Fe_2Al_5 phase takes place and releases heat supported by the DSC curve where a weak exothermic peak forms at 574 °C shown in Fig. 1. The formation of this compound is also predicted from its formation heat, which is −143.374 kJ/mol [26], and the heat generated by this reaction is not sufficient to induce the melting of aluminum. Increasing the sintering temperature to 650 °C, the Al phase disappears and the main phases are Fe_2Al_5, FeAl and a small amount of Fe. This is due to TE reaction in the temperature range between 600 and 650 °C. As described in Fig. 2, a sudden slope appears and the temperatures of specimen increase sharply to 1073 °C when the specimen is heated to the T_i, implying that the Al powders start to melt. The reactions between the solid Fe, Fe_2Al_5 and liquid Al are violent due to the liquid aluminum possessing a much higher reactivity than solid aluminum. The liquid aluminum phase quickly covers the iron surface by the capillary force owning to good wetting between Al liquid and Fe [27]. The large amount of heat releases from the formation of Fe_2Al_5 and FeAl in the Fe−Al system, which leads to an instant rise in the temperature−time profiles from the T_i to the T_c. After TE reaction, as the specimen contains Fe_2Al_5 together with residual Fe, further heating leads to the diffusion reaction between Fe_2Al_5 and Fe, resulting in the formation of FeAl compound that is more stable at higher temperatures [14]. Therefore, the dominant process is solid-state diffusion and the formation of FeAl by the reaction of Fe_2Al_5 with

Fe during the temperature from 700 to 1000 °C. As the temperature increases to 1000 °C, the pure phase FeAl is obtained as the final product after an additional homogenizing process.

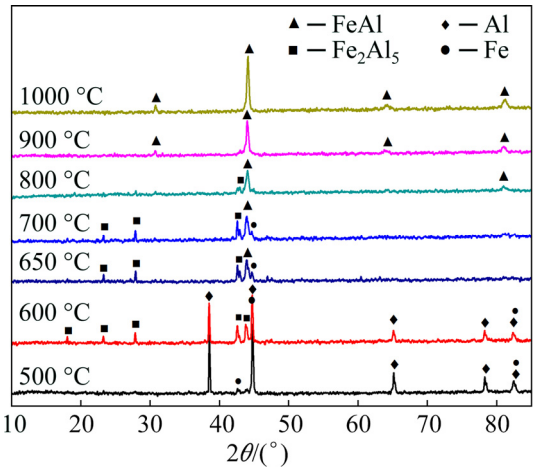

Fig. 3 XRD patterns of powder compacts synthesized at different final sintering temperatures from 500 to 1000 °C

3.3 Macrograph and pore structure

Figure 4 shows the macrographs of green compact and sintered porous Fe−Al intermetallics. The green compacts keep the integrated body. As can be seen, the specimen before sintering presents metallic sheen (Fig. 4(a)), and the specimens gradually become dark in colour with increasing the sintering temperature (Figs. 4(b)−(h)). At the same time, the specimens have a variety of macroscopic expansion with increasing sintering temperature because of the thermal explosion reaction, which significantly changes the size of the specimens. But all of the specimens keep the original cylindrical shape, no deformation and cracking are observed.

The optical metallographs of specimens are presented in Fig. 5, fully showing the internal pore structure of the porous material. As shown in Fig. 5, the black regions are pores, meanwhile the white regions represent intermetallics skeletons. It can be seen clearly that the porous materials are composed of interconnected skeleton, larger pores among skeletons and small pores in the interior of skeleton. The size of a number of large pores is about 100 μm, as shown in Fig. 5(b), while some small pores distribute in the interior of skeleton, with a size around 5 μm (Fig. 5(c)). Interconnected pores can be found easily that make porous material an open cellular structure as marked by red lines (Fig. 5). The observations are supported by the fracture micrographs of sintered specimens shown in Fig. 6. As it can be seen that for the specimen sintered at 650 °C, the skeletons consist almost entirely of numerous small particles accumulating together tightly or loosely and the pore distribution is non-uniform. With increasing sintering temperature, the large pores and the particle shape distribute more uniformly. Also, many pores exist in the products, as shown by red circles in Fig. 6, which have a complex porous structure.

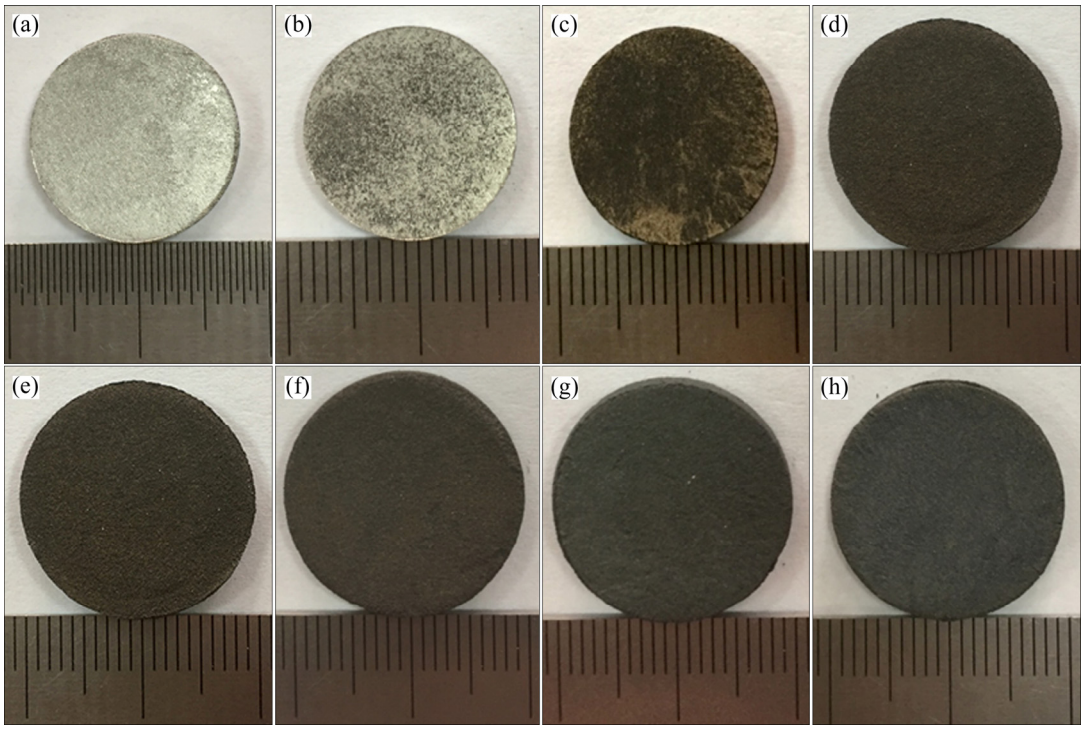

Fig. 4 Macrographs of green compact (a) and sintered specimens at 500 °C (b), 600 °C (c), 650 °C (d), 700 °C (e), 800 °C (f), 900 °C (g) and 1000 °C (h)

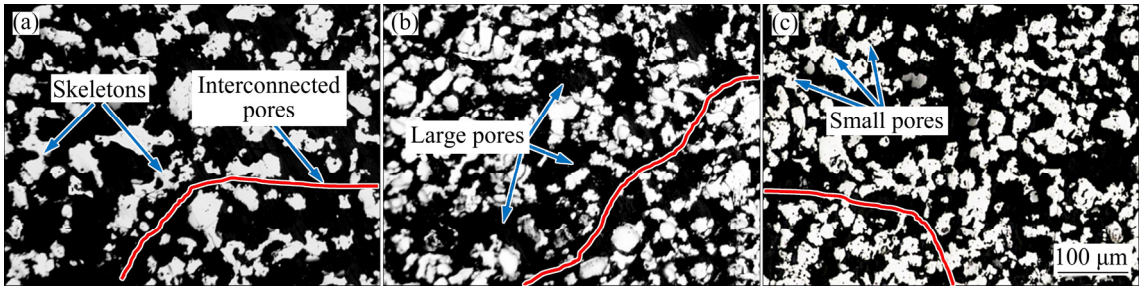

Fig. 5 Optical metallographs of specimens sintered at temperatures of 650 °C (a), 800 °C (b) and 1000 °C (c)

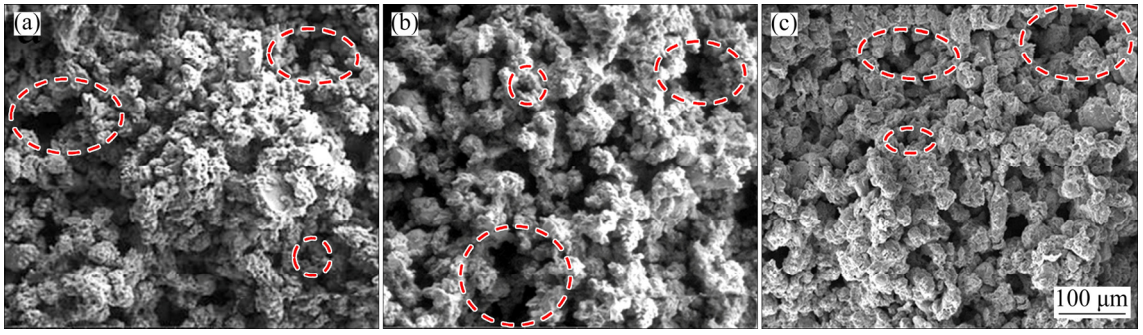

Fig. 6 SEM images of specimens sintered at temperatures of 650 °C (a), 800 °C (b) and 1000 °C (c)

3.4 Oxidation properties

Figure 7 shows the variation of the mass gain as a function of the time for porous Fe−Al materials oxidized at 650 °C for 96 h exposure in air. All of the oxidation kinetic curves exhibit parabolic-like behavior, indicating that the porous Fe−Al materials have good high-temperature oxidation resistance. The mass gains after 96 h reach the maximum values of 23.8496, 20.1437, 15.5332, 10.3185 and 2.4876 mg/cm^2, which correspond to the specimens sintered at 650, 700, 800, 900 and 1000 °C, respectively. Obviously, the mass gains decrease with increasing sintering temperature. In particular, the specimen prepared at 1000 °C shows the lowest mass gain compared with other four specimens, which exhibits better high-temperature oxidation resistance than the other four specimens. This is ascribed to the decrease of the residual Fe and the increase of the Fe−Al compound identified by XRD patters in Fig. 3. This is because the residual Fe is easily oxidized to form Fe_2O_3, which is not beneficial to the high temperature oxidation. Whereas, the Fe−Al compounds have a capacity of forming a passivated dense Al_2O_3 layer on the surface [28,29], which prevents the material from being oxidized. This ensures the longevity in service life and high accuracy in filtration of the material under rigorous environments.

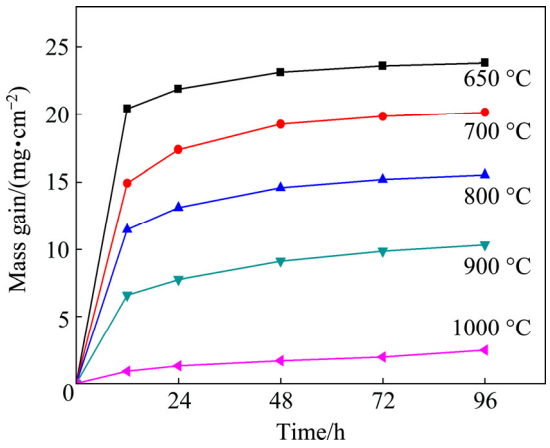

Fig. 7 Mass gain of porous Fe−Al monoliths sintered at different temperatures and further oxidized at 650 °C in air

3.5 Pore forming mechanism

The variation in porosity of porous Fe−Al with sintering temperature is shown in Fig. 8. The open porosities are measured to be 19.87%, 37.39%, 65.28%,

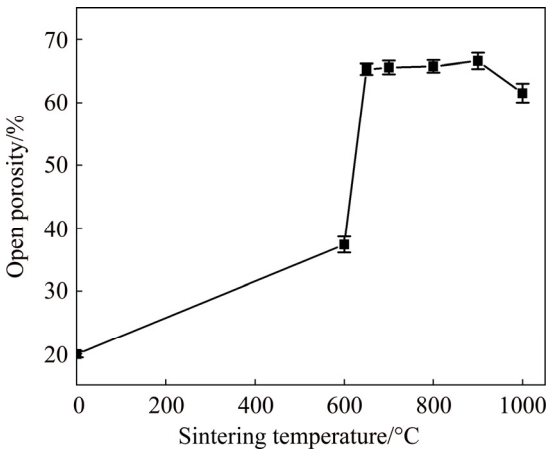

Fig. 8 Variation in open porosity of porous Fe−Al inter-metallics as function of sintering temperature

65.56%, 65.74%, 66.61% and 61.47%, corresponding to sintering temperatures of 0 (green compact), 600, 650, 700, 800, 900 and 1000 °C, respectively. It can be seen that the porosity of green compacts is 19.87%, which is due to the fact that green compacts formed by the cold-pressed method could not be fully dense and many pores exist among the Fe and Al powder particles. With the increase of the furnace temperature, the diffusion rate increases. Since the intrinsic diffusion coefficient of Fe is much smaller than that of Al, and some pores are caused by the Kirkendall effect [30] and a small amount of Fe_2Al_5 is formed. As a result, the open porosity of sintered specimen increases to 37.39% at 600 °C. Also, it can be seen that the open porosity of Fe−Al intermetallics sintered at 650 °C shows an abrupt increase, reaching 65.28%. The reason can be attributed to the TE reaction. During the TE procedure, Fe and liquid Al react violently, and the specimens release massive amount of heat, which forms a large number of the in-situ pores in the original aluminum particle sites because of the consumption of the aluminum. However, this result is not in an agreement with the observations made by GAO et al [14] who reported that these pores are mainly caused by the Kirkendall effect from 600 to 650 °C at a heating rate of 1 °C/min. In the present case, it takes only 5 min from 600 to 650 °C at a heating rate of 10 °C/min, the time for diffusion of the atoms is shorter, resulting in the limitation of Kirkendall effect. In addition, the chemical reaction rate is much faster than the diffuse rate at the reaction stage of liquid Al and Fe surface. The magnitude of former is strongly dependent on the temperature, but that of latter is insensitive [27]. This is because of an exponential relationship (Arrhenius equation) between the chemical reaction rate constant k and temperature T:

$$k=A\cdot\exp[-E/(RT)] \quad (1)$$

where A is the pre-exponential factor, R is the mole gas constant and E is the activation energy. However, there is a linearity relationship (Stokes−Einstein equation) between diffusion coefficient D and temperature T:

$$D=(RT/N)(1/2\pi r\eta) \quad (2)$$

where η is the viscosity, r is the radius of the spherical particle and N is Avogadro number. As shown in Fig. 8, the open porosity increases slowly with further increase in sintering temperature from 650 to 900 °C, but decreases slightly at 1000 °C. This can be explained by the fact that the dominant process is solid-state diffusion and the formation of FeAl by the reaction of Fe_2Al_5 with Fe after TE reaction, which is an additional homogenizing process. And the formation of FeAl is completed at 900−920 °C reported by GEDEVANISHVILI and DEEVI [26]. According to theory of sintering, after the synthesis of a single phase FeAl, the next step is the densification of the compact involving diffusion during the final stage of sintering. As a result, the porosity decreases slightly at 1000 °C.

Combined with the reaction mechanism in the Fe−Al system, we proposed a pore-formation model of the porous Fe−Al materials prepared by a thermal explosion reaction, as shown in Fig. 9.

1) The green compacts formed by the cold-pressed method could not be fully dense. Many pores exist among the Fe and Al powder particles inside the green compacts. In the present experiments, the porosity of the green compacts is measured to be 19.87%. Thus, there are many pores in the green compacts, which are the important sources for pores in the porous Fe−Al materials (Fig. 9(a)).

2) Before TE reaction, the Al diffusion rate increases with the increase of the furnace temperature, the intrinsic diffusion coefficient of Fe is much smaller, and some pores are caused by the Kirkendall effect, which forms a small amount of Fe_2Al_5 (Fig. 9(b)).

3) When the temperature increases to the T_i, the green compact is quickly ignited and the TE reaction occurs rapidly. Because of Al melting, there is good wetting between Al liquid and Fe, and Al liquid infiltrates into grain boundary of Fe and Fe_2Al_5 by the capillary force, which diffuses and reacts rapidly and continuously. In the meantime, some pores are from the precipitation of fine Fe−Al intermetallics particles. The net movement and consumption of Al results in a large number of in situ pores in the original Al particle sites (Fig. 9(c)).

4) After TE, FeAl intermetallics form the skeleton of the network structures of the porous monoliths, as shown in Fig. 5. In the final monoliths, there are mainly three structures, including FeAl intermetallics skeleton, large pores among skeletons and small pores in skeletons. At the same time, the in-situ pores combine with interstitial pore to form interconnected pores (Fig. 9(d)).

Compared with the traditional sintering to fabricate porous Fe−Al intermetallics, TE reaction is found to be more promising. The method of vacuum sintering takes longer sintering time (more than 5 h) [10,31,32] to prepare porous Fe−Al, which consumes a large amount of energy. TE reaction only takes less than 160 min (from room temperature to 1000 °C with a constant heating rate of 10 °C/min) to fabricate porous Fe−Al. The open porosity of TE specimens is slightly higher than results reported in Refs. [11,13,14]. Thus, the present work opens the way to synthesize high porosity Fe−Al intermetallics using an energy- and time-saving route.

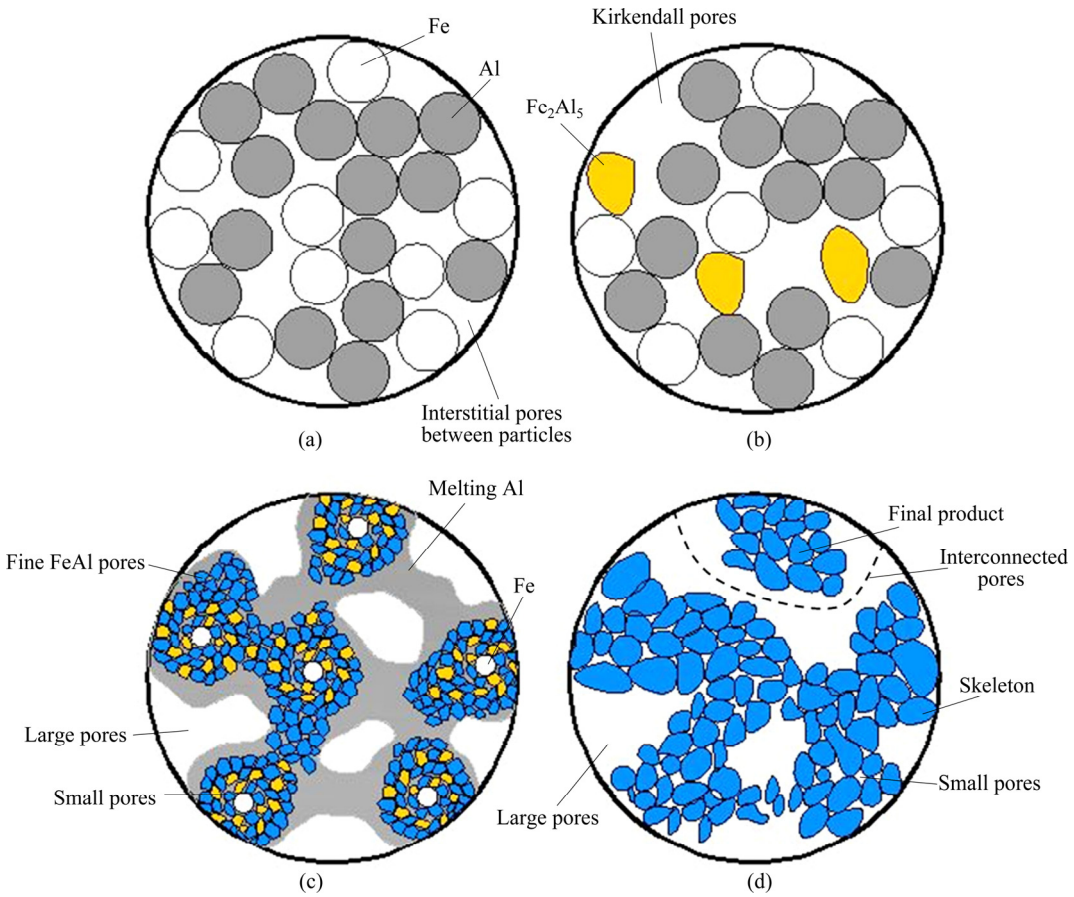

Fig. 9 Schematic diagram of pore-formation model of porous Fe−Al intermetallics: (a) Green compact; (b) Reacting front; (c) Reacting region; (d) Product

4 Conclusions

1) A time- and energy-saving sintering process with a heating rate of 10 °C/min is successfully conducted for fabricating FeAl-based intermetallics within 160 min. A TE reaction occurs at 636 °C and by increasing sintering temperature up to 1000 °C, FeAl is the dominated phase in the final products.

2) The obvious heat release phenomenon is observed, and all of the porous monoliths keep their original cylindrical shape and do not crack after the thermal explosion. The porous FeAl-based intermetallics possess a high open porosity of about 65%. At the same time, the porous materials show good high temperature oxidation resistance at 650 °C in air, especially the specimen sintered at 1000 °C.

3) The main pore formation mechanism includes the residual pores among the particles of the green powder compacts, and the in-situ pores owing to the molten aluminum particles flowing during the TE reaction. Large pores are formed by the interstitial pore combining with the in-situ pores, and the small pores are formed from the precipitation of Fe−Al intermetallics particles.

References

[1] MUTLU I. Synthesis and characterization of Ti−Co alloy foam for biomedical applications [J]. Transactions of Nonferrous Metals Society of China, 2016, 26: 126−137.

[2] HAMMEL E C , IGHODARO O L R, OKOLI O I. Processing and properties of advanced porous ceramics: An application based review [J]. Ceramics International, 2014, 40: 15351−15370.

[3] BANHART J. Manufacture, characterisation and application of cellular metals and metal foams [J]. Progress in Materials Science, 2001, 46: 559−553.

[4] LEFEBVRE L P, BANHART J, DUNAND D C. Porous metals and metallic foams: Current status and recent developments [J]. Advanced Engineering Materials, 2008, 10: 775−787.

[5] GAO Hai-yan, HE Yue-hui, ZOU Jin, XU Nan-ping, LIU C T. Tortuosity factor for porous FeAl intermetallics fabricated by reactive synthesis [J]. Transactions of Nonferrous Metals Society of China, 2012, 22: 2179−2183.

[6] AMAYA M, ESPINOSA-MEDINA M A, PORCAYO-CALDERON J, MARTINEZ L, GONZALEZ-RODRIGUEZ J G. High temperature corrosion performance of FeAl intermetallic alloys in molten salts [J]. Materials Science and Engineering A, 2003, 349: 12−19.

[7] ZHU Xiao-lin, YAO Zheng-jun, GU Xue-dong, CONG Wei, ZHANG Ping-ze. Microstructure and corrosion resistance of Fe−Al intermetallic coating on 45 steel synthesized by double glow plasma surface alloying technology [J]. Transactions of Nonferrous Metals Society of China, 2009, 19: 143−148.

[8] WANG Qian, LENG Xue-song, YANG Tian-hao, YAN Jiu-chun. Effects of Fe−Al intermetallic compounds on interfacial bonding of clad materials [J]. Transactions of Nonferrous Metals Society of China, 2014, 24: 279−284.

[9] CHOJNACKI M, JOZWIAK S, KARCZEWSKI K, BOJAR Z. Modification of Fe and Al elemental powders' sintering with addition of magnesium and magnesium hydride [J]. Intermetallics, 2011, 19: 1555−1562.

[10] LAZINSKA M, DUREJKO T, LIPINSKI S, POLKOWSKI W, CZUJKO T, VARIN R A. Porous graded FeAl intermetallic foams fabricated by sintering process using NaCl space holders [J]. Materials Science and Engineering A, 2015, 636: 407−414.

[11] KARCZEWSKI K, STEPNIOWSKI W J, CHOJNACKI M, JOZWIAK S. Crystalline oxalic acid aided FeAl intermetallic alloy sintering: Fabrication of intermetallic foam with porosity above 45% [J]. Materials Letters, 2016, 164: 32−34.

[12] KARCZEWSKI K, STEPNIOWSKI W J, JOZWIAK S. Highly-porous FeAl intermetallic foams formed via sintering with Eosin Y as a gas releasing agent [J]. Materials Letters, 2016, 178: 268−271.

[13] KARCZEWSKI K, STEPNIOWSKI W J, KZCZOR P, JOZWIAK S. Fabrication of Fe−Al intermetallic foams via organic compounds assisted sintering [J]. Materials, 2015, 8: 2217−2226.

[14] GAO Hai-yan, HE Yue-hui, SHEN Pei-zhi, ZOU Jin, XU Nan-ping, JIANG Yao, HUANG Bai-yun, LIU C T. Porous FeAl intermetallics fabricated by elemental powder reactive synthesis [J]. Intermetallics, 2009, 17: 1041−1046.

[15] SHI Quan-lin, QIN Bo-tao, FENG Pei-zhong, RAN Hua-shen, SONG Bin-bin, WANG Jian-zhong, GE Yuan. Synthesis, microstructure and properties of Ti−Al porous intermetallic compounds prepared by a thermal explosion reaction [J]. RSC Advances, 2015, 5: 46339−46347.

[16] MORSI K. Review: Reaction synthesis processing of Ni−Al intermetallic materials [J]. Materials Science and Engineering A, 2001, 299: 1−15.

[17] RAN H S, NIU J N, SONG B B, WANG X H, FENG P Z, WANG J Z, GE Y, AKHTAR F. Microstructure and properties of Ti_5Si_3-based porous intermetallic compounds fabricated via combustion synthesis [J]. Journal of Alloys and Compounds, 2014, 612: 337−342.

[18] YEH C L, SUN W E. Use of TiH_2 as a reactant in combustion synthesis of porous Ti_5Si_3 and Ti_5Si_3/TiAl intermetallics [J]. Journal of Alloys and Compounds, 2016, 669: 66−71.

[19] HOU Q Y. Microstructure and wear resistance of steel matrix composite coating reinforced by multiple ceramic particulates using SHS reaction of Al−TiO_2−B_2O_3 system during plasma transferred arc overlay welding [J]. Surface and Coatings Technology, 2013, 226: 113−122.

[20] WANG Z, JIAO X Y, FENG P Z, WANG X H, LIU Z S, AKHTAR F. Highly porous open cellular TiAl-based intermetallics fabricated by thermal explosion with space holder process [J]. Intermetallics, 2016, 68: 95−100.

[21] JIANG Y, HE Y H, XU N P. Effects of the Al content on pore structures of porous Ti−Al alloys [J]. Intermetallics, 2008, 16: 327−332.

[22] HU L, BENITEZ R, BASU S, KARAMAN I, RADOVIC M. Processing and characterization of porous Ti_2AlC with controlled porosity and pore size [J]. Acta Materialia, 2012, 60: 6266−6277.

[23] SINA H, CORNELISSON J, TURBA K, IYENGAR S. A study on the formation of iron aluminide (FeAl) from elemental powders [J]. Journal of Alloys and Compounds, 2015, 636: 261−269.

[24] LEE S H, LEE J H, LEE Y H, SHIN D H, KIM Y S. Effect of heating rate on the combustion synthesis of intermetallics [J]. Materials Science and Engineering A, 2000, 281: 275−285.

[25] KANG H Z, HU C T. Swelling behavior in reactive sintering of Fe−Al mixtures [J]. Materials Chemistry and Physics, 2004, 88: 264−272.

[26] GEDEVANISHVILI S, DEEVI S C. Processing of iron aluminides by pressureless sintering through Fe+Al elemental route [J]. Materials Science and Engineering A, 2002, 325: 163−176.

[27] ZHANG W, LIU Y, WANG H, WEI Q Q. Preparation and properties of porous Ti−Al alloys by reactive infiltration [J]. Powder Metallurgy, 2011, 54: 253−256.

[28] NOWAK K, KUPKA M. High-temperature oxidation behaviour of *B*2 FeAl based alloy with Cr, Zr and B additions [J]. Materials Chemistry and Physics, 2012, 132: 902−908.

[29] GUO Ping-yi, SHAO Yong, ZENG Chao-liu, WU Ming-fang, LI Wei-li. Oxidation characterization of FeAl coated 316 stainless steel interconnects by high-energy micro-arc alloying technique for SOFC [J]. Materials Letters, 2011, 65: 3180−3183.

[30] HE Yue-hui, JIANG Yao, XU Nan-ping, ZOU Jin, HUANG Bai-yun, LIU C T, LIAW P K. Fabrication of Ti−Al micro/nanometer-sized porous alloys through the Kirkendall effect [J]. Advanced Materials, 2007, 19: 2102−2106.

[31] SHEN P Z, SONG M, HE Y H, GAO H Y, ZOU J, XU N P, HUANG B Y, LIU C T. Synthesis and characterization of porous Fe−25wt.%Al alloy with controllable pore structure [J]. Powder Metallurgy and Metal Ceramics, 2010, 49: 3−4.

[32] CHEN Gang, CAO Peng, HE Yue-hui, SHEN Pei-zhi, GAO Hai-yan. Effect of aluminium evaporation loss on pore characteristics of porous FeAl alloys produced by vacuum sintering [J]. Journal of Materials Science, 2011, 47: 1244−1250.

热爆法制备 FeAl 基金属间化合物多孔材料

刘亚南[1,2]，孙 智[1]，蔡小平[1]，焦欣洋[1]，冯培忠[1]

1. 中国矿业大学 材料科学与工程学院，徐州 221116；2. 中国矿业大学 化工学院，徐州 221116

摘 要：以 Fe、Al 粉末为原料，采用热爆法制备 FeAl 基金属间化合物多孔材料，研究烧结温度对其相组成、孔结构以及抗氧化性能的影响。结果表明：Fe−Al 的热爆反应发生在 636 °C，1000 °C 烧结后得到单相 FeAl 金属间化合物多孔材料；多孔材料的开孔率达 65%，其主要由连续的颗粒骨架、骨架之间的大孔隙和骨架内部的小孔隙构成；孔隙主要来自粉末压坯颗粒之间存在的原始大孔隙、烧结过程中熔化的 Al 颗粒在毛细作用下发生流动形成的原位大孔隙以及析出过程中在 Fe−Al 产物颗粒之间形成的小孔隙。此外，FeAl 多孔材料在 650 °C 空气气氛中表现出较好的抗高温氧化性能。

关键词：Fe−Al 金属间化合物；多孔材料；热爆；相转变

(Edited by Wei-ping CHEN)